Progress In Electromagnetics Research M, Vol. 99, 211–221, 2021

A Conformal Quasi-Isotropic Dielectric Resonator Antenna for Wireless Capsule Endoscope Application

Beibei Xing, Yueyuan Zhang*, Hui Zou, and Zhiwei Liu

Abstract—A conformal quasi-isotropic dielectric resonator antenna (DRA) is first investigated for wireless capsule endoscope (WCE) application under the 5.8-GHz industrial, scientific, and medical (ISM) standard. The probe-fed hemispherical DRA (HDRA) is studied to match the shape of the spherical dome end, and the characteristic mode analysis (CMA) tool is applied to analyze the resonant modes of the proposed antenna to reveal the intrinsic behavior of the dielectric resonator. It is found that the quasi-isotropic radiation pattern can be achieved by combining HDRA's $TE_{111\sin\varphi}$ mode which radiates like a magnetic dipole and a small ground plane's TM_{10} mode that radiates like an electric dipole. In order to reach the requirement of 5.8 GHz in ISM, a ceramic hemispherical dielectric resonator with dielectric constant of 21.984 is investigated. The radius of the hemisphere is set to 5.35 mm. In free space, the measurement results show that the proposed antenna achieves 3.25% bandwidth, 86% maximum efficiency, and 7.2 dB gain deviation. The antenna is also measured in pork to approximate human body environment. The measurement results demonstrate that the antenna achieves 3.20% bandwidth, 8.15% maximum efficiency, and 9.0 dB gain deviation. Accordingly, the proposed antenna is suitable for WCE application at 5.8 GHz ISM standard.

1. INTRODUCTION

Wireless capsule endoscopy (WCE) systems instead of the traditional painful and discomfort gastrointestinal (GI) examination are used to capture images of the human digestive tract for medical applications. In this technique, the patient swallows a small capsule with an embedded camera. The capsule moves through the GI tract and records images, which are transmitted to a receiver unit outside the body of the patient. A physician interprets these images either in real time or offline [1, 2].

A variety of antennas for endoscopy have been proposed. For instance, Lee et al. proposed a wideband spiral antenna operating at 500 MHz with isotropic radiation pattern [3]. However, the antenna is placed at one end of the capsule, wasting the capsule's hemispherical space. In [4], a normal dipole is bended to obtain currents with three different orthogonal directions. The currents in different orientations provide polarization diversity characteristic, which can realize the orientation insensitive performance. Moreover, the antenna with an irregular is located in the middle of the capsule, taking up a large space inside the capsule. The shape of antenna is irregular. In addition, a gap antenna with an omnidirectional radiation pattern for WCE formed by a metal cylinder and a metal layer inside the capsule shell is proposed in [5].

The antennas above are either too large or take up too much space inside the capsule to leave enough space for other devices. The main reason is that the metal antenna structure is not flexible compared to the dielectric resonator antenna. With the improvement of people's health consciousness, implantable medical antenna to detect the health index is increasing, and the capsule antenna needs to transmit high resolution image. Therefore, implantable medical antenna demands higher spectrum

Received 19 September 2020, Accepted 26 November 2020, Scheduled 16 December 2020
* Corresponding author: Yueyuan Zhang (zyyaney1981@hotmail.com).
The authors are with the Department of Information Engineering, East China Jiaotong University, Nanchang 330013, China.

resource. However, traditional metal antenna such as patch antenna [6], loop antenna [7–9], and dipole antenna [10] is unable to meet the practical requirements very well in high frequency since the metal Ohm loss increases, and the radiation efficiency decreases. Maybe a dielectric resonator antenna would be a better choice. Moreover, the current researches on capsule antennas are mostly omnidirectional antennas with a radiation range of 180 degrees. The human digestive tract, especially small intestine, is winding. Due to unpredictable orientation of the capsule in gastrointestinal tract, omni-direction that has a radiation range of 180 degrees is an indispensable characteristic in WCE [5]. Nevertheless, quasi-isotropy that has a radiation range 360 degrees will be a better choice and will make the receiving more convenient in the case that the gain is sufficient. Therefore, a conformal quasi-isotropic dielectric resonator capsule antenna is proposed in this paper.

The DRA has alluring features such as small size, low loss, and high radiation efficiency. These attractive features make the DRA a good antenna candidate for WCE. High performance DRA mainly includes wide band [11], broadband circular polarization [12–14], miniaturization [15], and high gain [16, 17]. Like the metal filter antenna [22, 23], dielectric resonator antenna also has filtering characteristics by digging grooves in the floor, changing the feed, etc. Furthermore, the performance of the DRA can be improved by improving and innovating the shape and feed structure of the DRA. However, at present, the practical application of DRA is not wide enough. This paper introduces DRA into the medical field for the first time where DRA can give full play to its advantages. Moreover, compared with linear and planar antennas, DRA has greater margin of versatility and flexibility in material and shape. It can also be well conformed with the implantable medical antenna, such as the hemispherical dielectric resonator antenna. Accordingly, DRA is considered to be a potential candidate for the future of WCE. In recent years, HDRA has been widely studied, such as [18–20]. In this paper, a probe-fed HDRA with a small ground is proposed to WCE. Both ends of the capsule can be replaced by the proposed antenna, leading to more space for other devices inside the capsule antenna, such as micro camera, led, and wireless IC transmitter.

A comprehensive comparison between the proposed quasi-isotropic HDRA and some related designs is tabulated in Table 1. According to Table 1, quasi-isotropic antennas were realized in [24, 25], but they were not conformal with the capsule endoscope. Hemispherical DRAs were proposed in [19–21], but they were omnidirectional or unidirectional antennas. For the first time, the proposed antenna simultaneously obtains quasi-isotropic radiation patterns and conformal with capsule endoscope.

Table 1. Comparison between the proposed quasi-isotropic HDRA and the previous related antennas.

Ref.	ε_r	F_r	BW	antenna shape	Volume	Mode	Radiation
[19]	9.2	3.6	47%	HDRA	10.85	TE_{111}, TM_{101}	NM
[20]	9.2	2.3	75%	Inverted HDRA	34	TM_{101}, $HM_{10\delta}$	NM
[21]	9.2	4.55	29%	half HDRA	12	TM_{101} like	NM
[24]	10	2.4	7%	Rectangle	10.57	TE_{111}, TM_{10}	Isotropic
[25]	20	2.4	7%	Cylinder	9.92	$HEM_{11\delta}$, TM_{10}	Isotropic
This work	**21.984**	**5.8**	**3.20%**	**HDRA**	**0.641**	$\mathbf{TE_{111\,sin}}$, $\mathbf{TM_{10}}$	**Isotropic**

ε_r = dielectric constant, F_r = resonantfrequency (GHz), BW = bandwidth (GHz), Volume = volume occupied by the antenna (cm^3). The above is the comparison of the best cases from all references. NM = Not mentioned.

2. ANTENNA CONFIGURATION AND SIMULATION ENVIRONMENT

Quasi-isotropic DRA has been proposed for the first time in [24] which was a probe-fed rectangular DRA with small ground plane. It has been shown that the DR radiated like a magnetic dipole, and the small ground plane radiated like an electric dipole. By combining the two complementary dipoles in the DRA, a good quasi-isotropic radiation pattern was obtained. The next quasi-isotropic DRA was proposed

in [25], which was a microstrip-fed rectangular DRA. However, the shapes of the above two antennas cannot be conformal to the capsule. In order to apply the dielectric resonator to the capsule antenna while it adapts to the small size of the capsule, a hemispherical quasi-isotropic dielectric resonator antenna is presented for the first time in this paper, which can make full use of the hemispherical structure at both ends of the capsule antenna.

Figure 1 shows the configuration of the hemispherical DRA with a radius $r = 5.35$ mm and dielectric constant $\varepsilon_r = 21.984$. The DRA is fed by a 50 ohm coaxial probe of length l and diameter w, located at a displacement of from the center. A small circular ground plane is used in this antenna which works as an electric dipole. And it is printed directly on the base of hemispherical dielectric resonator. The diameter of the ground plane is comparable with that of the DRA but much smaller than the wavelength. The proposed antenna is a quasi-isotropic dielectric resonator antenna working at the 5.8-GHz ISM band. And a 50 ohm coaxial probe feed has the advantages of the further easy integration of a transceiver under the ground plane and less impact on the antenna's radiation performance [26]. Figs. 1(a), (b), Fig. 2(a) are the schematic view, bottom view, and top view of the proposed antenna, respectively. To prevent short circuits, leave a nonmetallic field with a diameter c around the probe. The distance from

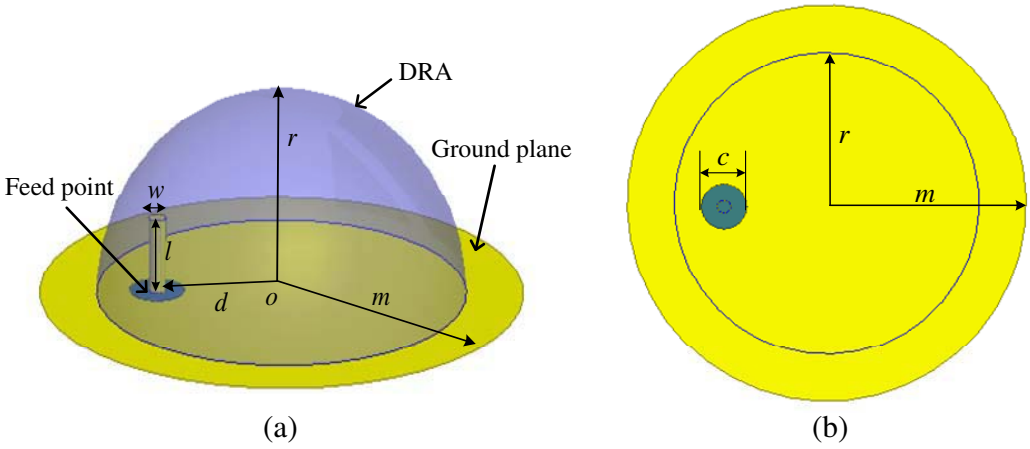

Figure 1. Configuration of the proposed quasi-isotropic DRA. (a) Schematic view, (b) bottom view. $r = 5.35$ mm; $m = 5.35$ mm, $d = 3.6$ mm; $l = 2.2$ mm; $w = 0.5$ mm; $c = 0.9$ mm.

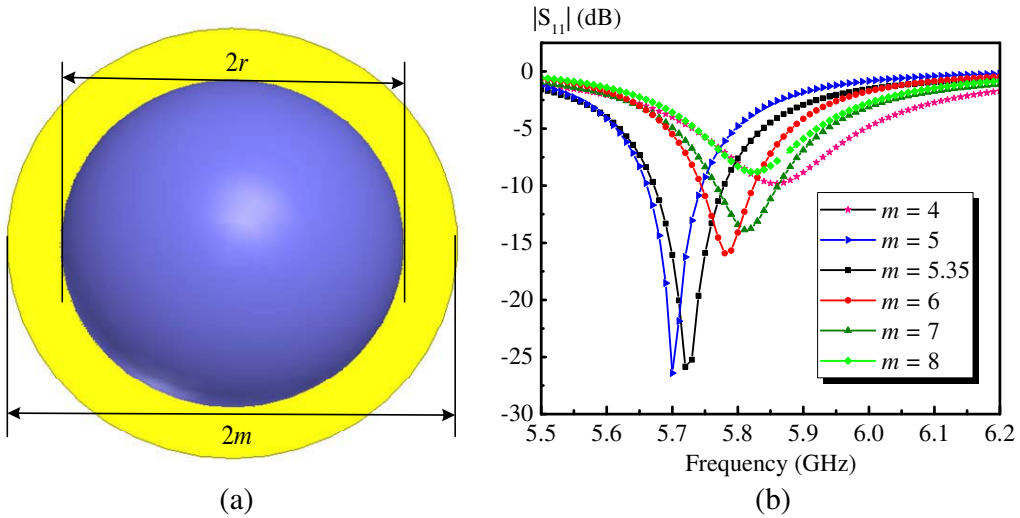

Figure 2. (a) Top view of the proposed quasi-isotropic DRA, (b) simulated reflection coefficient of the probe-fed HDRA for different ground plane radius.

the center of the sphere to the probe is d. The diameter of the probe is w. Detailed discussion about optimization of probe length and position can be seen in Section 3.

The DRA is fabricated using a titanium-magnesium K20 dielectric ceramics with a dielectric constant of $\varepsilon_r = 21.984$ and loss tangent of $\tan\delta < 0.0001$.

The resonant frequency of an HDRA is given by [21]:

$$f_r = \frac{4.775 \times 10^7 \mathrm{Re}(Ka)}{\sqrt{(\varepsilon_r)R}} \tag{1}$$

where "f" is the resonant frequency, "ε_r" the dielectric constant of the HDRA, "R" the radius of the hemisphere (in centimeters), and "Ka" the wavenumber in the dielectric.

The radiation pattern of the total field is dependent on the relative amplitudes of the magnetic and electric dipoles, which are affected by the dimensions of the DRA and ground plane, respectively. A parametric study was done using HFSS to study this in detail. The effect of ground-plane size is discussed. Fig. 2(b) shows the simulated reflection coefficients of the hemispherical DRA for different ground plane radii of $m = 4$, 5, 5.35, 6, 7, and 8 mm. The resonance frequency remains almost unchanged as the radius decreases from 8 mm to 6 mm. It is verified that the resonance is caused by the DRA.

However, as can be observed from the figure, the reflection coefficient is affected significantly as decreases further; the resonance frequency shifts upwards to 5.87 GHz when the radius is 4 mm. This significant frequency shift is caused by the fact that a good image of the DRA cannot be obtained from the ground plane when the ground plane size is not sufficiently large. By compare the corresponding elevation radiation patterns for 5 and 5.35 mm, it can be seen that the ground plane affects the pattern considerably.

The antenna mechanism is shown in Fig. 3. Two-dimensional coordinates are plotted on the graph. The resonances of the DR $\mathrm{TE}_{111\sin\varphi}$ mode are excited in the passband, radiating like a magnetic dipole along y axis in Fig. 3(a). The ground radiates as an electric dipole along x axis as shown in Fig. 3(b). The two are orthogonal to form a quasi-isotropic antenna.

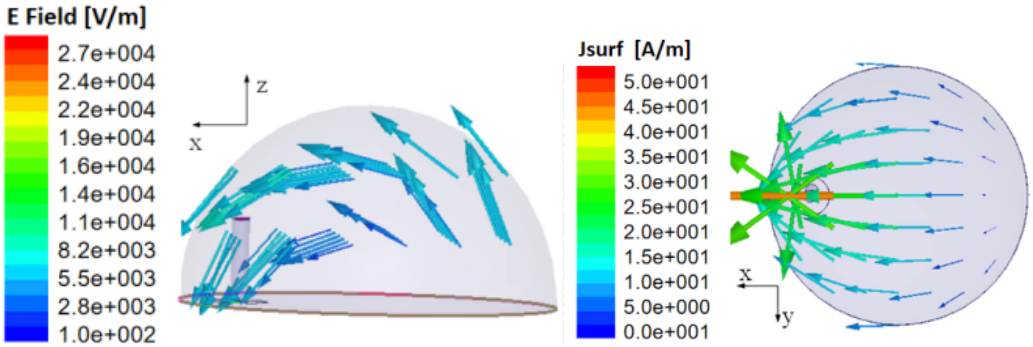

Figure 3. (a) Simulated current distribution on the ground plane at 5.8 GHz, (b) simulated E-fields inside the DRA at 5.8 GHz.

To save the simulation time and computer resource, reflection coefficient, input impendence, effect of electrical components, and biocompatible coating thickness are analyzed in free space.

3. ANTENNAS SIMULATION AND ANALYSIS

The simulated reflection coefficients for different probe lengths of $l = 1.8$, 2.0, and 2.2 mm are shown in Fig. 4. With reference to the figure, the probe length can be used to adjust the impedance level without changing the resonance frequency significantly, verifying that the resonance is caused by the DRA instead of the dipole mode of the probe. Simultaneously, the thickness w and position d of the probe are also simulated and analyzed. The simulation results show that the antenna performance is

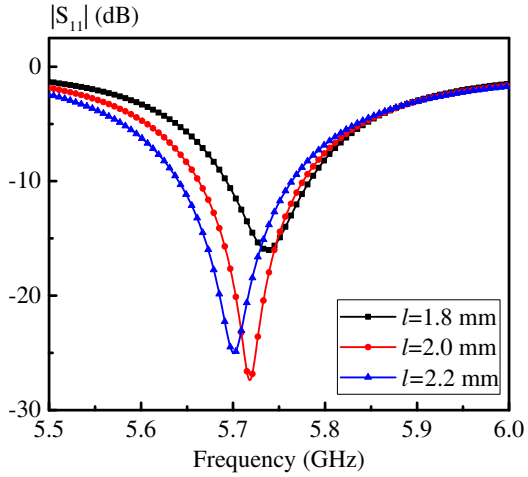

Figure 4. Simulated S-parameters for different probe lengths.

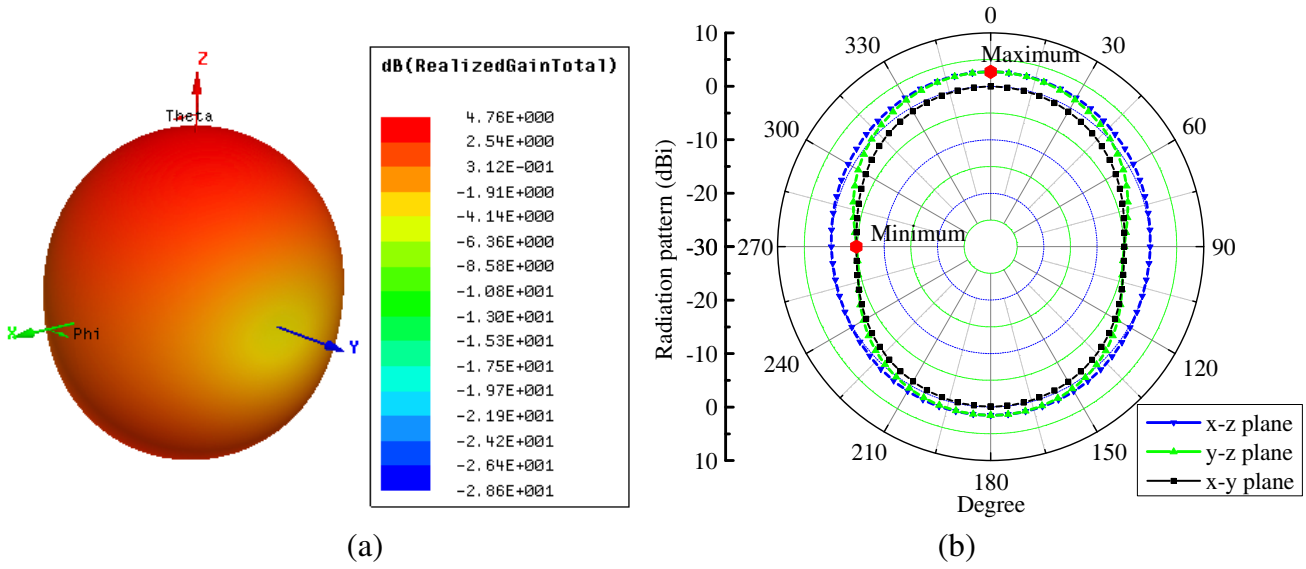

Figure 5. Fair field radiation pattern of the hemispherical DRA. (a) 3D pattern, (b) simulated radiation pattern at 5.7 GHz in the x-z plane, y-z plane and x-y plane.

not very sensitive to these parameters in a certain range, which brings great convenience to the antenna processing. Considering the brevity of the article, the simulation result diagram is not placed here.

To illustrate quasi-isotropic radiation, the 3D radiation pattern of the antenna is shown in Fig. 5(a). It is symmetrical in x-z plane, y-z plane, and x-y plane. From the 3D radiation pattern, we can see that gain is maximal in z-direction and minimal in y-direction. The maximum and minimum radiated power densities are 2.75 and -4.46 dBi, respectively. Consequently, the gain fluctuation is 7.21 dBi, smaller than another quasi-isotropic antenna [27]. Correspondingly, the maximum and minimum are marked with red dots in Fig. 5(b). It can be observed that the radiation patterns in the x-z plane, y-z plane, and x-y plane are quasi omnidirectional. The gain deviation is less than 7.3 dBi. Quasi-isotropic radiation is obtained over the entire spherical radiating surface, as expected.

The internal space of WCE is fully considered in this paper. As shown in Fig. 6, the antenna is placed on one end of the capsule, and other electrical components, such as RF transmitter, battery, LEDs, and camera, can be placed on the middle part of the capsule. In this communication, parylene-C with $\varepsilon_r = 2.95$ and $\tan\delta = 0.013$ as in [28] is considered as the biocompatible coating material in

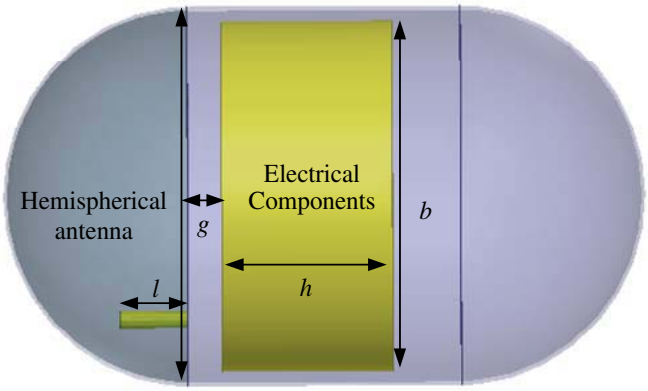

Figure 6. Antenna and electrical components in capsule.

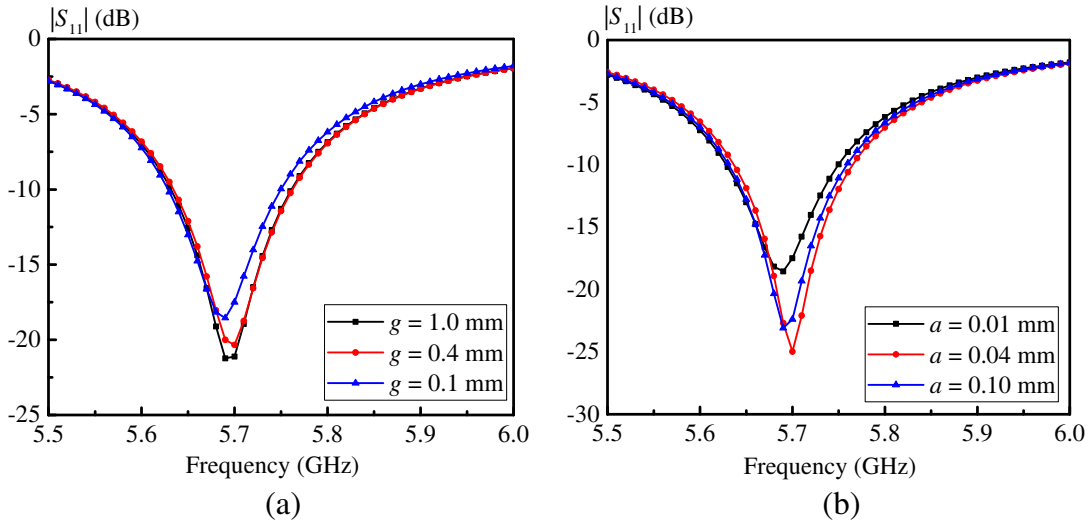

Figure 7. (a) S-parameters for different distance g between the electrical component and the antenna; (b) S-parameters for different coating thickness a.

this design. As show in Fig. 6, to verify the influence of these factors, a metal cylinder is used to simulate the electrical component. The distance g between the electrical component and the antenna is changed to analyze the influence. As show in Fig. 7(a), the S-parameter hardly changes with the distance shortened. It shows that the dielectric resonator antenna and metallic electrical component have good electromagnetic compatibility even in a small space, which is a great advantage over the metallic antenna for DRA applied to the capsule endoscope. When $g = 0.1$ mm, reflection coefficients of the antenna with different coating thicknesses a are studied in Fig. 7(b). It can be seen from the figure that the parameters only change slightly with the change of thickness. The stability of dielectric resonator antenna is cracking.

After debugging and optimization in free space, the antenna was placed in the gastric tissue ($\varepsilon_r = 56$ and $\sigma = 6.3$ in 5.8 GHz) to simulate the scene of stomach. The diameter of the sphere-shaped gastric tissue is 60–70 mm. To simulate the insufficient contact of the capsule in the stomach, a hollow ball with an outer radius of $r_1 = 30$ mm and inner radius of $r_2 = 10$ mm was used to simulate the scene of the capsule antenna placed in the human stomach. However, the return loss is lost. By adjusting the length of the probe l to 2 mm, the return loss can be improved well. The results are shown in Fig. 9(a). Even if $r_1 = 35$ mm, the return loss does not change compared with 30 mm. To compare the scenes of free space and stomach, the impedance offered by this antenna is investigated, as said in [29]. There is no change in the impedance other than the resonant frequency as shown in Fig. 8. Comparing Fig. 8(a)

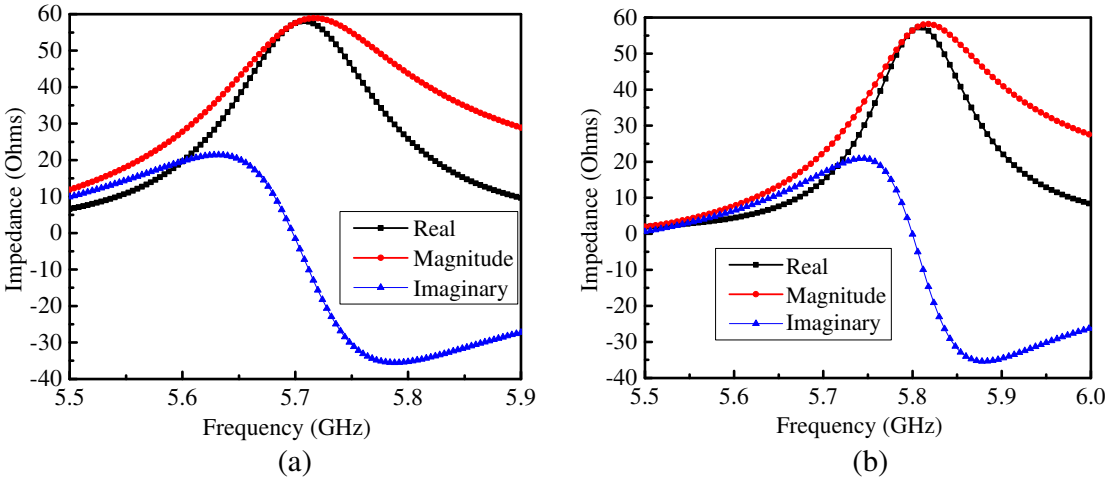

Figure 8. Plot of the real, imaginary and magnitudes in ohms of the impedance offered at the input (a) the impedance in free space, (b) the impedance in simulative stomach.

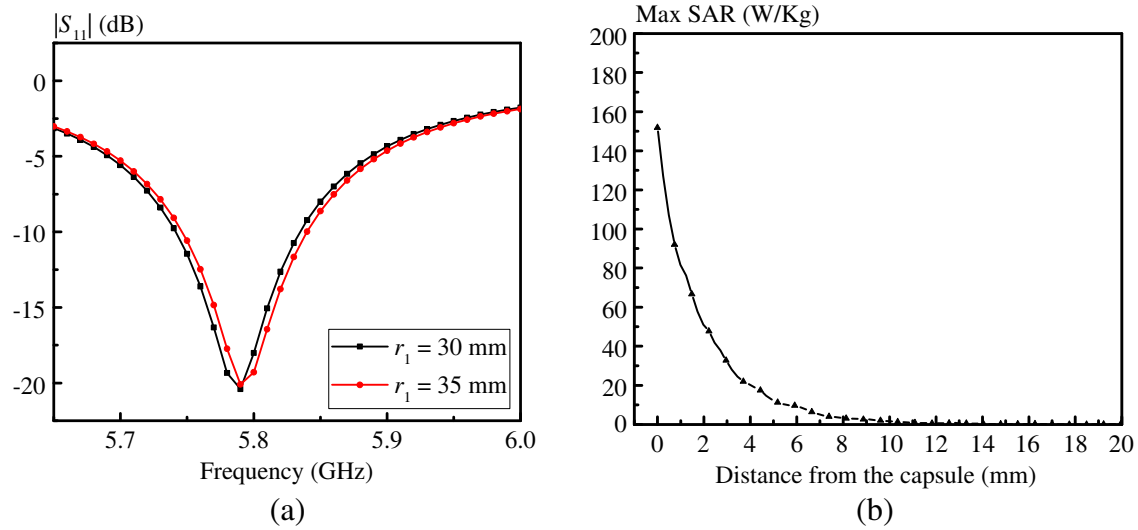

Figure 9. (a) S-parameters for different thickness r_1 of simulated stomach; (b) 1-g average SAR values from the inner wall to outer wall of the stomach at 5.8 GHz (1 W input power for normalization).

and Fig. 8(b), the resonant frequency is only slightly offset, indicating that the dielectric resonator antenna is relatively stable in human digestive tract.

In conclusion, when the antenna is placed in the simulative stomach, the resonant frequency of the antenna is 5.8 GHz, and the bandwidth covers ISM band 5.725–5.875 GHz. In addition, when the size of the stomach is changed, the resonant frequency does not change, as Shown in Fig. 9(a). Compared with the simulation in free space, the frequency of the antenna is shifted by 0.1 GHz, indicating that the dielectric resonator antenna is very stable in human body, which is one of the reasons that the dielectric resonator antenna is more suitable for capsule endoscopy than the metal antenna.

Safety consideration of the human body should also be discussed, and specific absorption rate (SAR) is calculated in a stomach model. According to the IEEE standard limitations, the maximum 1-g average SAR should be less than 1.6 W/kg while the maximum 10-g average SAR should not exceed 2 W/kg. Fig. 9(b) shows 1-g average SAR values from the inner wall to outer wall of the stomach when the input power of the proposed capsule antenna is 1 W, and max 1-g average SAR is 150 W/kg. Away from the antenna, the SAR values drop rapidly. In order to meet the peak 1-g SAR standard limitations

of IEEE (1.6 W/kg), the antenna can deliver a maximum power of 10 mW. This indicates that the SAR value of the dielectric resonator antenna is within a very reasonable range.

4. MEASUREMENT AND DISCUSSION

The physical picture of the proposed antenna is shown in Fig. 10. The antenna is fed by 50 ohm coaxial cable, and feed networks are unnecessary. In Fig. 11, the coaxial cable's length is 100 mm, which is soldered to the antenna. The coaxial core is inserted into the DRA as a coaxial probe to feed, and the coaxial outer core is welded to the small ground. The whole device is inserted into minced pork for measurement. The measurement is performed by vector network analyzer Rhode & Schwarz ZVA 67. Due to the similar electromagnetic characteristics of pork and human body [30], pork mince was used to replace the actual stomach. The performance of the antenna is tested under two environments, free space and pork mince. The antenna efficiency of measurement in free space can reach up to 86%, and the measurement gain deviation 7.7 dBi is a bit poor compared with simulation result 7.2 dBi, which is because dielectric is inhomogeneous. The S-parameters comparison between simulation and measurement is shown in the Fig. 12. It can be seen that test bandwidth of the antenna has become wider, which may be caused by the increase of load resistance R_L caused by the coaxial connection between the test port and the antenna. It is expressed as:

$$Q = \frac{X}{R_r + R_L} = \frac{f}{BW} \tag{2}$$

where R_L is the load resistance, R_r the radiation resistance, X the imaginary part of the impedance associated with radiation by the antenna, BW the antenna bandwidth, and f the resonant frequency.

Figure 10. Physical picture of the proposed antenna.

Figure 11. S-parameters measurement in minced pork.

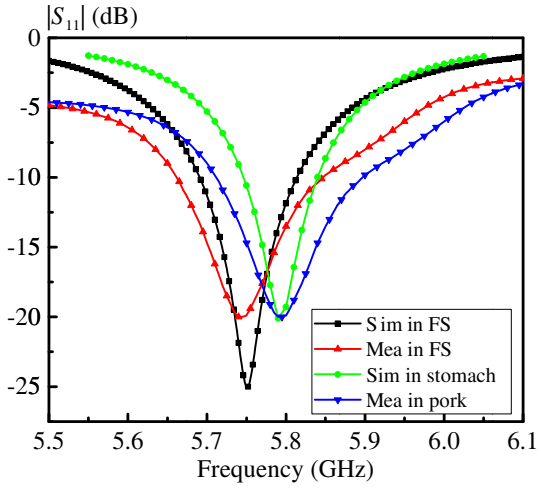

Figure 12. Comparison between simulation and measurement in free space (FS) and stomach.

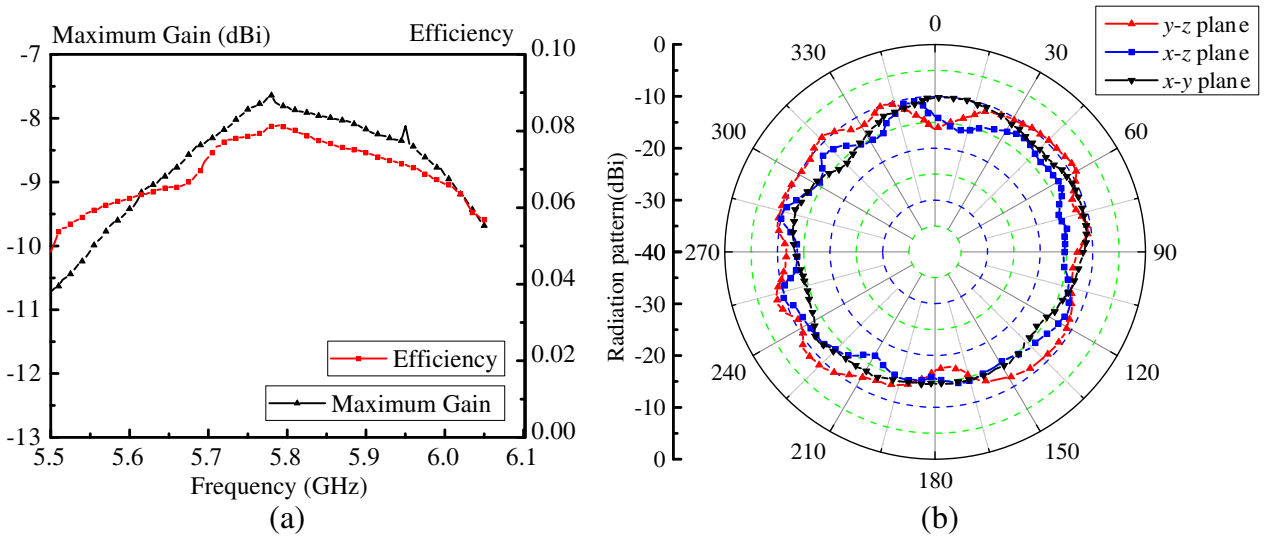

Figure 13. Measurement results in the pork (a) maximum gain and efficiency in pork mince, (b) radiation pattern at 5.8 GHz in the x-z plane, y-z plane and x-y plane in pork mince.

Besides, the resonant frequency is offset after the pork is added, which is basically consistent with the simulation results. The parameters such as the efficiency, gain, and radiation pattern are also tested in simulating stomach of pork mince. As shown in Fig. 13, the efficiency and gain are pretty good compared with metal WCE antenna. The maximum efficiency can reach 8% in Fig. 13(a). Measured radiation pattern can be seen in Fig. 13(b), and the gain deviation is 9 dBi.

5. CONCLUSION

A conformal hemispherical quasi-isotropic dielectric resonator antenna for wireless capsule endoscope is first investigated in this paper. A hemispherical dielectric resonator with a circular ground plane is used to form the $TE_{111\sin\varphi}$ mode and the TM_{10} mode at 5.8 GHz. The radiation pattern of the $TE_{111\sin\varphi}$ mode is almost the same as a magnetic dipole, and the TM_{10} mode can be considered as an electric dipole. Combination of the two modes can achieve the quasi-isotropic radiation pattern. Compared with other metal capsule endoscope antennas, the dielectric resonator antennas have higher radiation efficiency and more stable performance. In order to simulate the environment in stomach, the proposed antenna is measured in minced pork. The measurement results show that the bandwidth is 3.20%; radiation efficiency is 8.15%; and the gain deviation is 9 dBi. Moreover, the property of quasi-isotropic pattern can be observed from the measured results obviously. As a result, our proposed antenna is a suitable design for WCE application under ISM standard.

ACKNOWLEDGMENT

This work was supported by Jiangxi provincial Outstanding Youth Talent Project of Science and Technology Innovation (No. 20192BCBL23003) and Natural Science Foundation of Jiangxi Province (No. 20202BAB202004).

REFERENCES

1. Yun, S., K. Kim, and S. Nam, "Outer-wall loop antenna for ultrawideband capsule endoscope system," *IEEE Antennas and Wireless Propagation Letters*, Vol. 9, 1135–1138, 2010.

2. Miah, M. S., A. N. Khan, C. Icheln, et al., "Antenna system design for improved wireless capsule endoscope links at 433 MHz," *IEEE Transactions on Antennas and Propagation*, Vol. 67, No. 4, 2687–2699, 2018.
3. Lee, S. H., J. Lee, Y. J. Yoon, S. Park, and S. Nam, "A wideband spiral antenna for ingestible capsule endoscope systems: Experimental results in a human phantom and a pig," *IEEE Transactions on Biomedical Engineering*, Vol. 58, No. 6, 1734–1741, 2011.
4. Li, Y., Y. X. Guo, and S. Xiao, "Orientation insensitive antenna with polarization diversity for wireless capsule endoscope system," *IEEE Transactions on Antennas and Propagation*, Vol. 65, No. 7, 3738–3743, 2017.
5. Duan, Z., L.-J. Xu, S. Gao, and W. Geyi, "Integrated design of wideband omnidirectional antenna and electronic components for wireless capsule endoscopy systems," *IEEE Access*, Vol. 6, 29626–29636, 2018.
6. Cui, W., R. Liu, L. Wang, et al., "Design of wideband implantable antenna for wireless capsule endoscope system," *IEEE Antennas and Wireless Propagation Letters*, Vol. 18, No. 12, 2706–2710, 2019.
7. Wang, J., M. Leach, E. G. Lim, et al., "An implantable and conformal antenna for wireless capsule endoscopy," *IEEE Antennas and Wireless Propagation Letters*, Vol. 17, No. 7, 1153–1157, 2018.
8. Lei, W. and Y. X. Guo, "Design of a dual-polarized wideband conformal loop antenna for capsule endoscopy systems," *IEEE Transactions on Antennas and Propagation*, Vol. 66, No. 11, 5706–5715, 2018.
9. Shang, J. and Y. Yu, "An ultrawideband capsule antenna for biomedical applications," *IEEE Antennas and Wireless Propagation Letters*, Vol. 18, No. 12, 2548–2551, 2019.
10. Li, Y., Y. X. Guo, and S. Xiao, "Orientation insensitive antenna with polarization diversity for wireless capsule endoscope system," *IEEE Transactions on Antennas and Propagation*, Vol. 65, No. 7, 3738–3743, 2017.
11. Abedian, M., S. K. A. Rahim, and M. Khalily, "Two-segments compact dielectric resonator antenna for UWB application," *IEEE Antennas and Wireless Propagation Letters*, Vol. 11, 1533–1536, 2012.
12. Liu, S., D. Yang, Y. Chen, et al., "Broadband dual circularly polarized dielectric resonator antenna for ambient electromagnetic energy harvesting," *IEEE Transactions on Antennas and Propagation*, Vol. 68, No. 6, 4961–4966, 2020.
13. Zhou, Y. D., Y. C. Jiao, Z. B. Weng, et al., "A novel single-fed wide dual-band circularly polarized dielectric resonator antenna," *IEEE Antennas and Wireless Propagation Letters*, Vol. 15, 930–933, 2015.
14. Pan, Y. M. and K. W. Leung, "Wideband omnidirectional circularly polarized dielectric resonator antenna with parasitic strips," *IEEE Transactions on Antennas and Propagation*, Vol. 60, No. 6, 2992–2997, 2012.
15. Lee, M. T., K. M. Luk, K. W. Leung, et al., "A small dielectric resonator antenna," *IEEE Transactions on Antennas and Propagation*, Vol. 50, No. 10, 1485–1487, 2002.
16. Al-Alem, Y. and A. A. Kishk, "Wideband millimeter-wave dielectric resonator antenna with gain enhancement," *IEEE Antennas and Wireless Propagation Letters*, Vol. 18, No. 12, 2711–2715, 2019.
17. Petosa, A. and S. Thirakoune, "Rectangular dielectric resonator antennas with enhanced gain," *IEEE Transactions on Antennas & Propagation*, Vol. 59, No. 4, 1385–1389, 2011.
18. Mukherjee, B., P. Patel, and J. Mukherjee, "A review of the recent advances in dielectric resonator antennas," *Journal of Electromagnetic Waves and Applications*, Vol. 34, No. 9, 1095–1158, 2020.
19. Mukherjee, B., P. Patel, and J. Mukherjee, "Hemispherical dielectric resonator antenna based on apollonian gasket of circles — A fractal approach," *IEEE Transactions on Antennas and Propagation*, Vol. 62, No. 1, 40–47, Jan. 2014, doi: 10.1109/TAP.2013.2287011.
20. Mukherjee, B., P. Patel, and J. Mukherjee, "A novel cup-shaped inverted hemispherical dielectric resonator antenna for wideband applications," *IEEE Antennas and Wireless Propagation Letters*, Vol. 12, 1240–1243, 2013.

21. Mukherjee, B., P. Patel, G. S. Reddy, and J. Mukherjee, "A novel half hemispherical dielectric resonator antenna with array of slots for wideband applications," *Progress In Electromagnetics Research C*, Vol. 36, 207–221, 2013.
22. Choudhary, D. K. and R. K. Chaudhary, "Compact filtering antenna using asymmetric CPW-fed based CRLH structure," *AEU — International Journal of Electronics and Communications*, Vol. 126, 2020.
23. Choudhary, D. K. and R. K. Chaudhary, "Vialess wideband bandpass filter using CRLH transmission line with semi-circular stub," *II International Conference on Microwave & Photonics, ICMAP-2015*, IEEE, 2016.
24. Pan, Y. M., K. W. Leung, and K. Lu, "Compact quasi-isotropic dielectric resonator antenna with small ground plane," *IEEE Transactions on Antennas and Propagation*, Vol. 62, No. 2, 577–585, 2014.
25. Hu, P. F., Y. M. Pan, X. Y. Zhang, et al., "A compact quasi-isotropic dielectric resonator antenna with filtering response," *IEEE Transactions on Antennas and Propagation*, Vol. 67, No. 2, 1294–1299, 2018.
26. Liu, C., Y. X. Guo, and S. Xiao, "Circularly polarized helical antenna for ISM-band ingestible capsule endoscope systems," *IEEE Transactions on Antennas and Propagation*, Vol. 62, No. 12, 6027–6039, 2014.
27. Su, Z., K. Klionovski, R. M. Bilal, and A. Shamim, "A dual bandadditively manufactured 3D antenna on package with near-isotropic radiation pattern," *IEEE Transactions on Antennas and Propagation*, Vol. 66, No. 7, 3295–3305, Apr. 2018.
28. Duan, Y.-X. Guo, M. Je, and D.-L. Kwong, "Design and in vitro test of a differentially fed dual-band implantable antenna operating at MICS and ISM bands," *IEEE Transactions on Antennas and Propagation*, Vol. 62, No. 5, 2430–2439, May 2014.
29. Mukherjee, B. and A. Raj, "Investigation of a hemispherical dielectric resonator antenna for enhanced bandwidth of operation," *International Journal of Applied Electromagnetics & Mechanics*, Vol. 41, No. 4, 457–466, 2013.
30. Zhang, K., C. Liu, X. Liu, et al., "A conformal differentially fed antenna for ingestible capsule system," *IEEE Transactions on Antennas and Propagation*, Vol. 66, No. 4, 1695–1703, 2018.